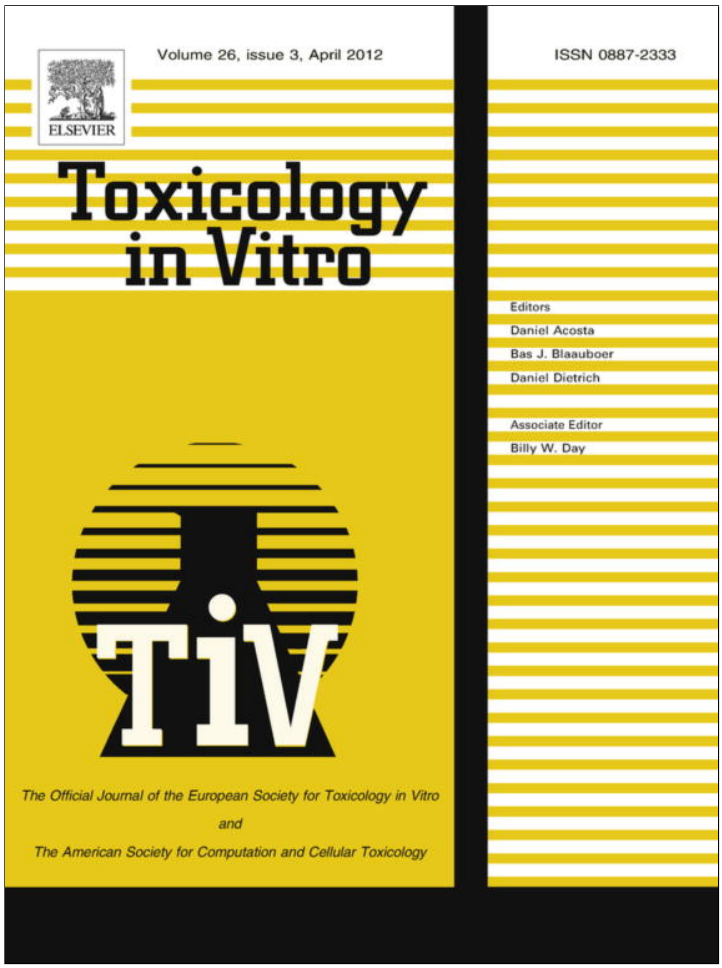

Toxicology in Vitro 26 (2012) 493–499

Contents lists available at SciVerse ScienceDirect

Toxicology in Vitro

journal homepage: www.elsevier.com/locate/toxinvit

Inhibitory effects of pectenotoxins from marine algae on the polymerization of various actin isoforms

Suzanne C. Butler [a], Christopher O. Miles [b], Amna Karim [a], Michael J. Twiner [a,*]

[a] Department of Natural Sciences, University of Michigan–Dearborn, Dearborn, MI 48128, USA
[b] Section for Chemistry and Toxicology, Norwegian Veterinary Institute, Oslo, Norway

ARTICLE INFO

Article history:
Received 28 November 2011
Accepted 22 December 2011
Available online 3 January 2012

Keywords:
Actin
Cytoskeleton
Depolymerization
Pectenotoxins
Phycotoxin
Polymerization

ABSTRACT

Pectenotoxins (PTXs) are marine toxins produced by dinoflagellates and which accumulate in shellfish. There are at least 14 different analogs of PTX with slight variations in structure leading to different chemical properties and consequently different toxicities. Since preliminary studies have shown that the parent compound PTX1 targets actin, we investigated the effects of two analogs, PTX2 and PTX2 seco acid, on the polymerization and depolymerization of skeletal muscle actin, smooth muscle actin, cardiac muscle actin, and non-muscle actin. Optimized actin assays using fluorescently labeled skeletal muscle actin and SDS–PAGE were jointly used to determine the relative amounts of filamentous and globular actin formed during polymerization and depolymerization experiments. Our findings suggest that PTX2 causes a dose-dependent decrease in both the rate and yield of skeletal muscle actin polymerization (IC_{50} values of 44 and 177 nM; respectively), with no significant effects on depolymerization. Moreover, the inhibitory effects of PTX2 are conserved towards other actin isoforms (i.e., smooth muscle, cardiac muscle, and non-muscle), as the inhibitory effects on actin polymerization were also observed with similar IC_{50} values (range: 19–94 nM). No inhibitory effects on polymerization were observed for PTX2 seco acid, suggesting an intact lactone ring is necessary for bioactivity.

1. Introduction

In addition to okadaic acid (OA) and dinophysistoxins (DTXs), toxins associated with diarrhetic shellfish poisoning (DSP), several species of the dinoflagellate genus *Dinophysis* also produce pectenotoxins (PTXs). These toxins can accumulate in shellfish and present a potential human health hazard. *Dinophysis* toxins have been found throughout the world, including the US, Australia, Japan, New Zealand, and several European countries (EFSA, 2009). Of the PTXs, at least 14 analogs have been identified, with PTX2 being the main analog produced in algae (Fig. 1). PTXs produced in algae (e.g., PTX11) or through the metabolism of PTX2 by shellfish (e.g., PTX1, PTX3, and PTX6) retain the polyether macrolactone structure but are oxidized to varying degrees, except for PTX2 seco acid (PTX2-SA) where the lactone ring has been opened by enzymatic hydrolysis (Fig. 1).

Several PTX analogs are acutely toxic towards mice following intraperitoneal (*i.p.*) injection. These include PTX1, PTX2, PTX3, PTX4, PTX6, and PTX11 with acute LD_{50} or minimum lethal dose values ranging between ~200 and 770 μg/kg (Miles et al., 2004; Suzuki et al., 2006; Yasumoto et al., 1985; Yoon and Kim, 1997). Symptomatic animals appeared lethargic, had difficulties in breathing, lacked muscle coordination, and experienced cyanosis. Post-mortem histological analysis indicated liver pathology and changes in the spleen and kidney (Munday, 2008). Analogs of PTX7, PTX8, PTX9, and PTX2-SA are not acutely toxic, with toxicity values in excess of 5000 μg/kg (Miles et al., 2004; Sasaki et al., 1998). The Scientific Panel on Contaminants in the Food Chain has set a human acute reference dose (ARfD) of 0.8 μg/kg PTX2 equivalents (EFSA, 2009) that was based on animal data including intestinal toxicity studies using PTX2 in mice following oral administration (Ishige et al., 1988; Ito, 2006). The current European regulatory limit is 160 μg/kg OA equivalents per kilogram of shellfish meat, presumably based on the fact that OA and PTX are both produced by *Dinophysis* and therefore occur together. OA and DTXs have a different mechanism of action, as they are potent inhibitors of protein phosphatases (Bialojan and Takai, 1988; Takai et al., 1992), whereas PTX2 has no known inhibitory activity towards protein phosphatase 2a (Fladmark et al., 1998). Probability estimates that take into account both average consumption and

Abbreviations: ARfD, acute reference dose; APB, actin polymerization buffer; CI, confidence intervals; DSP, diarrhetic shellfish poisoning; DTX, dinophysistoxin; IC_{50}, 50% inhibitory concentration; OA, okadaic acid; PTX, pectenotoxin; SDS–PAGE, sodium dodecyl sulfate–polyacrylamide gel electrophoresis.

* Corresponding author. Address: Department of Natural Sciences, University of Michigan–Dearborn, 4901 Evergreen Rd., Dearborn, MI 48128, USA. Tel.: +1 313 593 5298; fax: +1 313 593 4937.
E-mail address: mtwiner@umd.umich.edu (M.J. Twiner).

0887-2333/$ - see front matter © 2011 Elsevier Ltd. All rights reserved.
doi:10.1016/j.tiv.2011.12.015

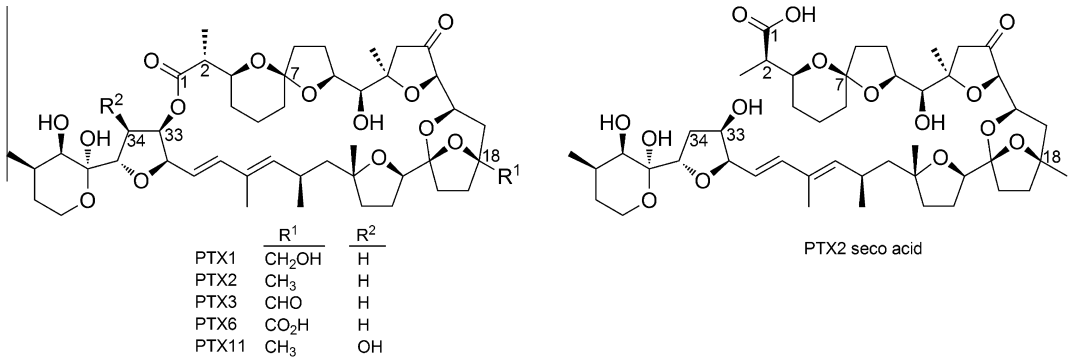

	R^1	R^2
PTX1	CH_2OH	H
PTX2	CH_3	H
PTX3	CHO	H
PTX6	CO_2H	H
PTX11	CH_3	OH

Fig. 1. Structure of selected PTXs (left) and PTX2 seco acid (right).

toxin concentration find a very small chance (0.2%) of exceeding the ARfD for PTXs. There have been no reported cases of human illness caused by PTXs, although their co-occurrence with OA makes it difficult to determine whether they contribute to or complicate DSP events (EFSA, 2009).

Studies of PTX1 in mice revealed liver damage (Terao et al., 1986) and *in vitro* studies with hepatocytes showed cytoskeletal disruption (Zhou et al., 1994). Subsequently, PTX2 was found to inhibit skeletal actin polymerization (Hori et al., 1999). Although comprehensive structure–activity studies are still lacking, studies of various cell types exposed to a few PTX analogs have found similar results. For example, PTX6 was found to cause F-actin depolymerization in neuroblastoma cells (Leira et al., 2002) and PTX2 caused actin depolymerization in hepatocytes (Espina and Rubiolo, 2008), intestinal cells (Ares et al., 2005) and neuroblastoma cells (Ares et al., 2007). However, PTX2 was rapidly metabolized in hepatocytes (Sandvik et al., 2004) suggesting some of the activity observed *in vitro* may be due to metabolites. X-ray crystal studies along with fluorescent skeletal muscle actin and SDS–PAGE studies suggested that PTX2 disrupts lateral contacts in F-actin filaments, capping the barbed end of a growing F-actin strand, but not severing filaments (Allingham et al., 2007).

Actin is a highly conserved protein found in nearly all eukaryotes, and plays a pivotal role in the cytoskeleton and muscle. Actin can exist as either monomeric G-actin (globular) or polymerized F-actin (filamentous). When the G-actin concentration is above a critical level, it spontaneously polymerizes to F-actin in the presence of 50–150 mM KCl and 1–2 mM $MgCl_2$, while the presence of Ca^{2+}, as $CaCl_2$, raises the critical concentration such that the G-actin form is favored (Khaitlina, 2001). Actins are classified as α, β, or γ in order of increasing basicity that results from variation among the acidic residues at the *N*-terminus (Khaitlina, 2001) while different tissues display differences among these types. Mammalian cardiac α-actin differs from skeletal α-actin at 4 out of 375 residues, while smooth muscle α-actin differs at 8 residues. Cytoplasmic β and γ actins differ from skeletal α-actin at 25 and 24 residues, respectively, while there are only four differences between cytoplasmic β-actin and γ-actin. Although there is a high degree of residue similarity between the actin isoforms, they cannot be interchanged for one another. Actin is the binding site for numerous toxins such as PTX, the marine toxins reidispongiolides and sphinxolides that sever and cap actin filaments (Allingham et al., 2005), and of the fungal toxin phalloidin that inhibits actin filament depolymerization (Cooper, 1987). According to Allingham et al. (2007), PTX2 has two contact sites with skeletal muscle actin at positions 175 (isoleucine) and 177 (arginine). Although all actin isoforms are conserved at these specific positions, there is variability amongst the isoforms at position 176 that may indirectly influence the binding kinetics of PTX.

It is well known that small structural changes in toxin and/or target (i.e., protein) can have profound effects on the affinity and efficacy of the toxin. Since all PTX inhibition studies to date have only utilized skeletal muscle actin, we sought to better understand these inhibitory relationships by assessing the effects of PTX2 and PTX2 seco acid on the four major actin isoforms (skeletal, cardiac, smooth muscle, non-muscle). These findings will be essential for interpreting *in vivo* exposures where PTXs that are systemically distributed will likely come into contact with all of these actin isoforms.

2. Material and methods

2.1. Toxin isolation

PTX2 was isolated from a natural bloom of *Dinophysis acuta* and was converted to PTX2-SA (Miles et al., 2004). Aliquots of toxins were stored dry at −20 °C and dissolved in methanol prior to use. Toxins were determined to be >95% pure by NMR and showed <1% impurity of other PTX analogs by liquid chromatography–mass spectrometry (LC–MS).

2.2. Reagents and proteins

All purified actin isoforms (>99% pure) were purchased from Cytoskeleton, Inc. (Denver, CO). Non-labeled and fluorescent pyrene-labeled skeletal muscle actin were purified (>99%) from rabbit skeletal muscle. Cardiac actin from bovine heart muscle was composed of 84% $\alpha_{cardiac}$ and 16% $\alpha_{skeletal}$ actin isoforms and smooth muscle actin from chicken gizzard consisted of ~80% γ_{smooth} muscle and 20% $\beta_{cytoplasmic}$ actin. Non-muscle actin from human platelets was composed of 85% β-actin and 15% γ-actin. All reagents, unless specified otherwise, were purchased from Sigma (St. Louis, MO).

2.3. Fluorescent skeletal muscle actin assays

Polymerization of skeletal muscle actin was determined using an actin polymerization assay according to the manufacturers protocol (cat. #BK003, Cytoskeleton Inc., Denver, CO). This assay is based on the enhanced fluorescence of pyrene-conjugated actin that occurs during polymerization when pyrene G-actin (monomer) forms pyrene F-actin. Fluorescence was measured using a BMG FluoStar (Durham, NC) microplate reader (excitation/emission 350/410 nm). To ensure that experiments started with only actin monomers, the initial G-actin (5.1 μM, or 0.2 mg/ml) in "G-buffer" consisting of 5 mM Tris–HCl pH 8.0, 0.2 mM $CaCl_2$, and 0.2 mM ATP was kept on ice for one hour to depolymerize any previously formed filaments and then centrifuged (13,000*g* at 4 °C for 30 min) to sediment any remaining oligomers. The G-actin monomer supernatant (100 μL per well) was incubated with various

concentrations of PTX2 or PTX2-SA (5–500 nM) or vehicle control (1% methanol) for 30 min at 37 °C after which polymerization was stimulated by the addition of 10 μL of actin polymerization buffer (APB) containing 500 mM KCl, 20 mM $MgCl_2$, and 10 mM ATP. Fluorescence was measured every minute for at least 90 min following polymerization stimulation. For each PTX concentration, at least three independent, replicate experiments were performed and data were normalized to the maximum fluorescence of the methanol control. The linear rate of actin polymerization was calculated over the 5 min immediately following the addition of APB while the polymerized yield was calculated by the averaged fluorescence between 70 and 90 min post-APB.

Depolymerization of skeletal muscle was tested in a similar manner. Pyrene-conjugated skeletal muscle actin (23 μM) in G-buffer with 4% APB was allowed to polymerize for 60 min at 25 °C. Depolymerization was initiated by diluting the reaction mixture 4-fold with G-buffer. Actin was distributed in 96-well plates and fluorescence was measured for 3 min to establish a baseline. Two concentrations of PTX2 or PTX2-SA (100 or 500 nM) or vehicle controls (1% methanol) were then added and fluorescence was measured every minute for at least 90 min. Phalloidin (2.3 μM), a fungal toxin known to inhibit actin depolymerization, was included as a positive control. Phalloidin tightly binds with filamentous actin at Cys-374 close to the C-terminus, inducing cross-linking with neighboring filaments and stabilizing the polymer against shearing stress and depolymerization (Faulstich et al., 1993).

2.4. Actin assays using SDS–PAGE

Since fluorescence-based assays were not available for the other actin isoforms, polymerization of cardiac muscle, smooth muscle, and non-muscle actin was determined by semi-quantitative SDS–PAGE (sodium dodecyl sulfate–polyacrylamide gel electrophoresis) methods, optimized in parallel with skeletal muscle actin. As with the fluorescent skeletal muscle actin, the initial G-actin (9.3 μM) in G-buffer was allowed to depolymerize on ice for 60 min and then centrifuged (13,000*g* at 4 °C for 30 min) to sediment any remaining oligomers. Supernatant (18 μL) was distributed into microcentrifuge tubes and incubated with various concentrations of PTX2 or PTX2-SA (5–500 nM) or vehicle control (1% methanol) at 25 °C for 30 min and APB was added to stimulate polymerization. Based on the fluorescent actin assay, polymerization was complete after 60 min and samples were centrifuged (*ca.* 16,000*g* at 25 °C for 60 min) to separate the polymerized F-actin (pellet) from the monomeric G-actin (supernatant). Both the pellet and supernatant were analyzed with SDS–PAGE, using precast gels with a 4% stacking layer and 12% resolving layer (Bio-Rad; cat. #456–1043). Equal volume samples (15 μL) were prepared with sample buffer (1:1 sample to buffer ratio) according to Laemmli (1970), loaded onto the gel, run at 200 V for ~40 min, and visualized with Coomassie Blue. Gel images were taken with either a Kodak EDAS 290 Electrophoresis Documentation and Analysis System or a Kodak Gel Logic 100 Imaging System. All images were analyzed with Kodak MI software v.4.0.3 and intensity values were calculated via summation of the background-subtracted pixel values in the band rectangle.

2.5. Statistics

Unless stated otherwise, all data from three or more independent experiments were illustrated as mean ± SE or mean with 95% confidence intervals (CI). Inhibition data were fitted to a four-parameter model, $Y = Y_{min}+(Y_{max}-Y_{min})/(1 + 10^{\log(IC50)-\log(concentration)\times Hill\ Slope})$ using GraphPad Prism (ver. 5.0c, San Diego, CA). Data were statistically compared using one-way ANOVA with Dunnett's post-test using GraphPad InStat version 3.0a (GraphPad, San Diego, CA) where $p < 0.05$ was considered significant.

3. Results

3.1. Effects of PTX analogs on fluorescent skeletal muscle actin polymerization

Actin polymerization was monitored using a fluorescent, pyrene actin based assay. Following the addition of ABP (used to stimulate polymerization at 35 min), polymerization of skeletal actin as indicated by fluorescence rapidly increased and then plateaued

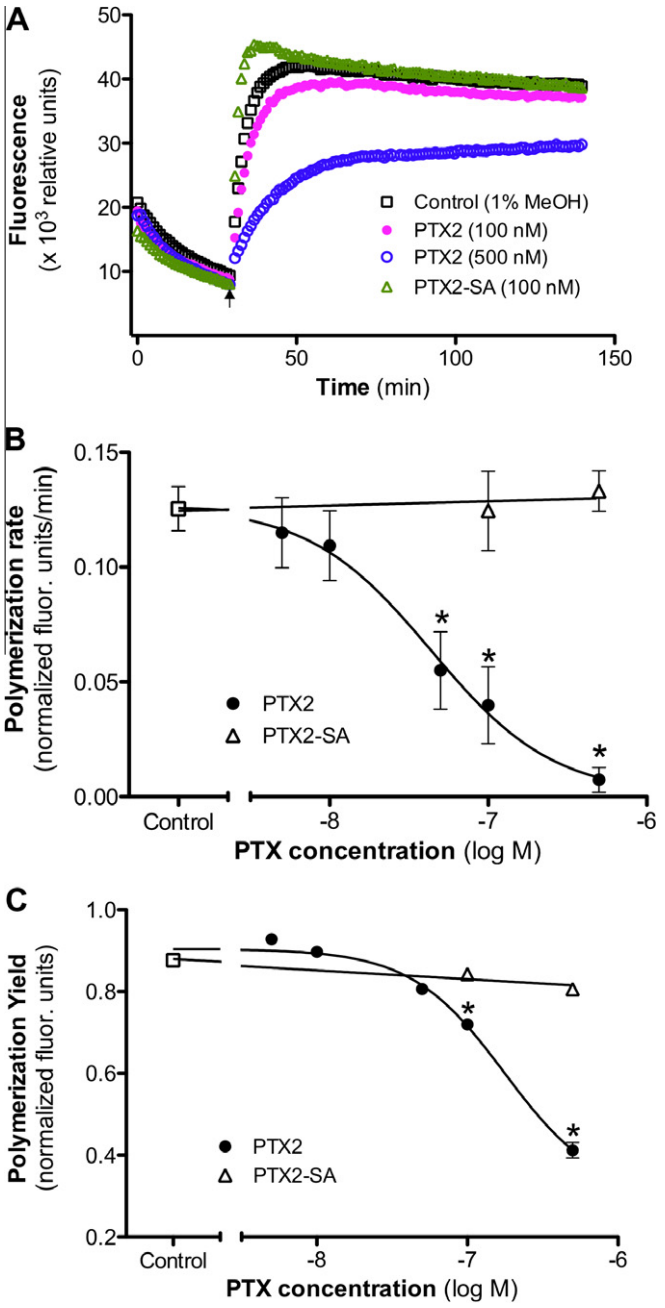

Fig. 2. Effects of PTX2 and PTX2-SA on skeletal actin polymerization using a fluorescence-based assay. (A) Representative traces of G-actin (not fluorescent) polymerized to F-actin (fluorescent) stimulated by the addition of actin polymerization buffer. Inhibition of the (B) rate and (C) yield of actin polymerization in the presence of various concentrations of PTXs (PTX2 and PTX2-SA). Rate and yield values (mean ± SE, $n \geqslant 3$) are calculated from fluorescence data normalized to the maximum fluorescence of the methanol control, with the corresponding yield IC_{50} value presented in Table 1. Absence of error bars in Panel C indicates they are smaller than the symbol. Data points indicated with an asterisk (*) are significantly different from control ($p < 0.05$).

Table 1
IC_{50} values for the inhibition of actin polymerization by PTXs.[a]

Actin isoform	IC_{50} (nM) (95% confidence interval)	
	PTX2	PTX2-SA
Skeletal muscle	32 (14–73)[b]	>500
Cardiac muscle	52 (30–91)	>500
Smooth muscle	19 (2–165)	>500
Non-muscle	94 (50–180)	>500

[a] All values were determined by SDS–PAGE assays at 60 min following the initiation of polymerization.
[b] IC_{50} value of 177 (6 to >500) nM as determined using the pyrene fluorescence assay.

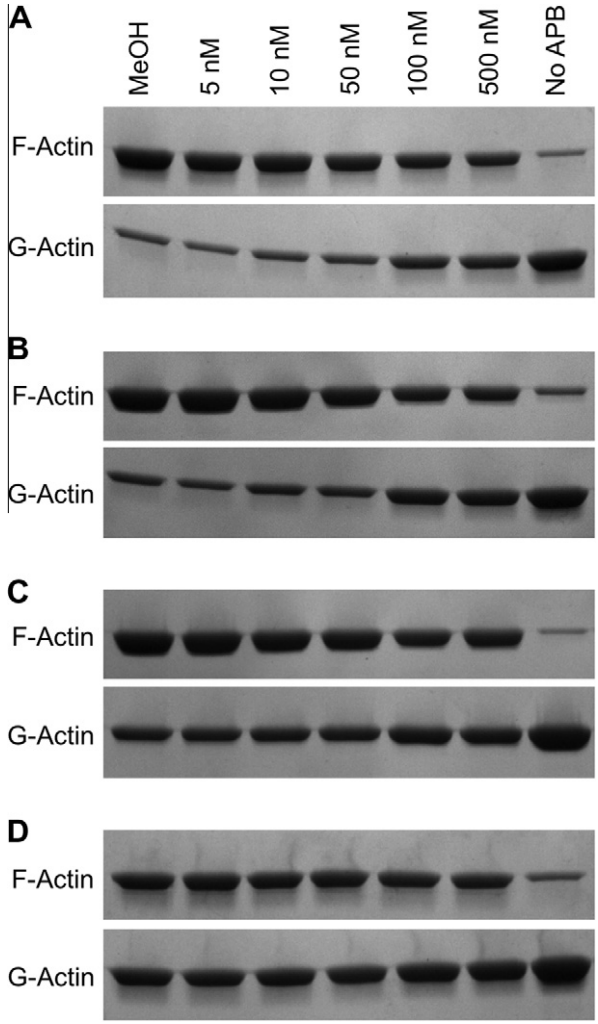

Fig. 3. Effects of PTX2 on polymerization of various actin isoforms using SDS–PAGE. Representative gel images of F-actin and G-actin are illustrated for (A) skeletal, (B) cardiac, (C) smooth, and (D) non-muscle actin 60 min after addition of actin polymerization buffer in the presence of various concentrations of PTX2. The last lane (''No APB'') corresponds to the unpolymerized starting material. Calculated band intensity ratios of F-actin:G-actin from replicated experiments were used to plot data illustrated in Fig. 4.

after 15 to 40 min (Fig. 2A). Representative traces of polymerizing actin in the presence of 100 and 500 nM PTX2, 100 nM PTX2-SA, or vehicle control (1% methanol) are illustrated. No significant effects were observed by the presence of 1% methanol relative to controls without vehicle (data not shown). The presence of PTX2 appeared to cause a decrease in both the rate and final yield of polymerized actin whereas PTX2-SA did not appear to have this effect. From replicated experiments, the rate of skeletal actin polymerization in vehicle controls was 0.125 ± 0.01 fluorescence units/min (Fig. 2B). However, in the presence of increasing concentrations of PTX2, the rates of polymerization were significantly reduced in a concentration-dependent manner to 0.01 ± 0.01 (500 nM PTX2) fluorescence units/min ($p < 0.05$). In contrast, PTX2-SA did not significantly alter the linear rate of polymerization (0.133 ± 0.009). PTX inhibitory concentration (IC_{50}) values on rate of polymerization (expressed as means with 95% confidence intervals) were 44 (21–89) nM for PTX2 and >500 nM for PTX2-SA (Fig. 2B and Table 1).

Increasing concentrations of PTX2 significantly reduced the final yields of polymerized actin, whereas PTX2-SA did not have any inhibitory effect at concentrations up to 500 nM (Fig. 2C). PTX inhibitory concentration (IC_{50}) values on actin yield (expressed as means with 95% confidence intervals) were 177 (6 to >500) nM for PTX2 and >500 nM for PTX-SA (Fig. 2C). The additional 'bump' following the initial rapid polymerization stage seen in Fig. 2A was not typical of PTX-2SA treatments, although it may be explained by a difference in fluorescence among ATP hydrolysis states (Brooks and Carlsson, 2008).

3.2. Effects of PTX analogs on skeletal, cardiac, smooth, and non-muscle actin polymerization

Since reliable fluorescence assays were not available for the other isoforms of actin, semi-quantitative SDS–PAGE was used to assess the inhibitory effects of the PTXs. Representative gel images showing F-actin- and G-actin-band intensities for skeletal, cardiac, smooth muscle, and non-muscle following treatment with increasing concentrations of PTX2 are illustrated in Fig. 3. As clearly shown for all actin isoforms, the ratio of F-actin to G-actin was inversely proportional to PTX2 concentration. Replicated experimental data (mean ± SE, $n \geqslant 3$) are illustrated in Fig. 4. Skeletal, cardiac, smooth, and non-muscle actin all exhibited a decreasing trend in actin polymerization with increasing PTX2 concentration. The calculated IC_{50} values for each actin isoform were not significantly different from each other and ranged between 19 and 94 nM (Table 1). In contrast, PTX2-SA did not significantly alter the polymerization of any of the actin isoforms at concentrations up to 500 nM (Fig. 4; Table 1). No significant effects were observed by the presence of 1% methanol relative to controls without vehicle (data not shown).

3.3. Effects of PTX analogs on fluorescent skeletal muscle actin depolymerization

Skeletal F-actin was exposed to two concentrations of PTX2 and PTX2-SA (100 and 500 nM) and depolymerization was monitored via F-actin fluorescence decay (Fig. 5A). Neither PTX analog significantly affected skeletal actin depolymerization relative to the controls (Fig. 5B). In contrast, phalloidin, a bicyclic peptide from mushrooms, was used as a positive control.

4. Discussion

This study has focused on characterizing the inhibitory effects of two PTX analogs on the activities of various actin isoforms. We have found that PTX2, the most potent PTX analog *in vivo* (Miles et al., 2004), caused a concentration-dependent decrease in both rate and yield of skeletal muscle actin polymerization and, for the first time, these inhibitory effects were also demonstrated for all other actin isoforms. These studies may prove to be helpful for correctly interpreting *in vivo* toxicological data and assessing PTX's anti-cancer potential (Kim et al., 2011).

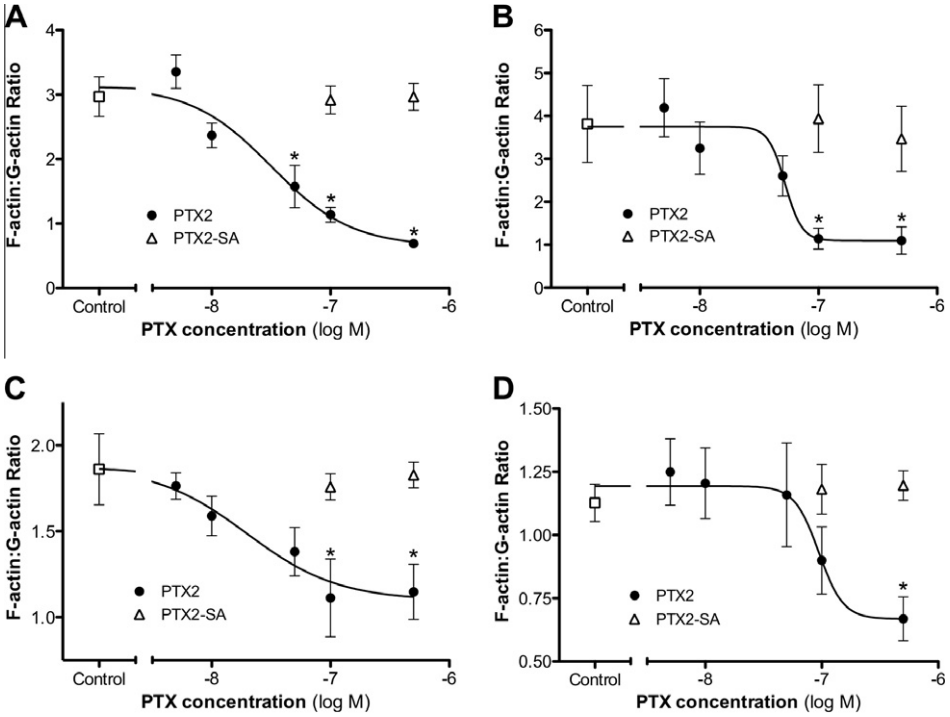

Fig. 4. Effects of PTX2 and PTX2-SA on the polymerization of various actin isoforms using SDS–PAGE. Plots show ratios of F-actin to G-actin (mean ± SE, $n \geqslant 3$) for (A) skeletal muscle, (B) cardiac muscle, (C) smooth muscle, and (D) non-muscle actin in the presence of various concentrations of PTX2 and PTX2-SA. Data points indicated with an asterisk (∗) are significantly different from control ($p < 0.05$). Note: Due to limited availability, 500 nM PTX2-SA data are from duplicate experiments ($n = 2$) only.

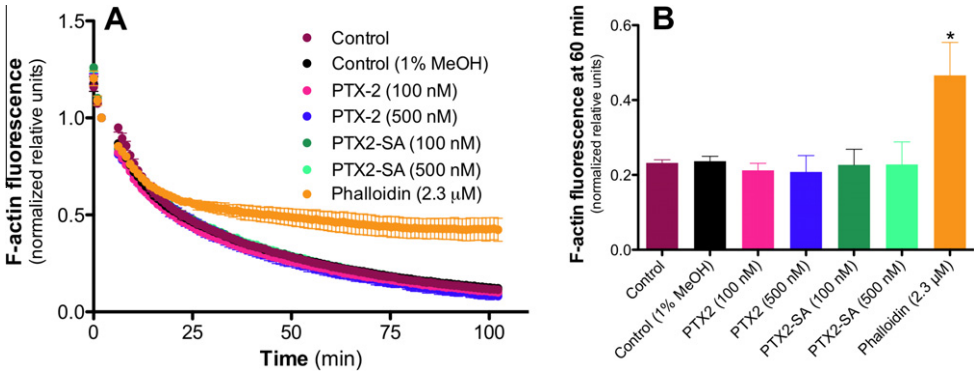

Fig. 5. Effects of PTX2 and PTX2-SA on skeletal F-actin depolymerization using a fluorescence-based assay. (A) Depolymerization of F-actin (fluorescent) to G-actin (not fluorescent) was monitored in the presence of various concentrations of PTX2, PTX2-SA, phalloidin (a known inhibitor of actin depolymerization), or vehicle control (methanol). Test substances were added 3 min after depolymerization was initiated and data were normalized to the point of addition. (B). F-actin fluorescence after 60 min. All data are presented as mean ± SE ($n = 3$). Data points indicated with an asterisk (∗) are significantly different from vehicle control ($p < 0.05$).

Polymerization of all actin isoforms was significantly inhibited in a concentration-dependent manner by PTX2, however, the degree of the responses slightly varied. By employing both fluorescent assays and SDS-gel techniques, polymerization of skeletal actin was significantly inhibited at PTX2 concentrations ⩾50 nM (−7.3 logM). Yield IC_{50} values as determined by the two methods were 177 and 32 nM, respectively. These levels of inhibition are qualitatively similar to other studies investigating skeletal actin and PTX2. For example, the seminal mechanistic study of Hori et al. (1999) used 2.7 μM actin and found that 300 nM PTX2 inhibited the rate and yield of polymerization to *ca.* 15% and 60% of the control; respectively. More recently, Allingham et al. (2007) using 9 μM actin found that 1 μM PTX2 inhibited to similar levels.

Polymerization of cardiac, smooth muscle, and non-muscle actin were each inhibited by PTX2 with IC_{50} values that closely mirrored the IC_{50} value for skeletal actin using the same method. The similar responses are not necessarily surprising since there is a high degree of amino acid sequence conservation between the four tested actin isoforms and none of these differences directly correspond to the proposed PTX binding sites at positions 175 and 177 (Allingham et al., 2007). In particular, both skeletal muscle and cardiac muscle isoforms are α-actin with 98.9% (371/375) amino acid sequence similarity and a non-polar methionine occupying position 176 (Khaitlina, 2001) between the two proposed PTX binding sites. Furthermore, the source of cardiac actin was known to consist of ∼16% skeletal α-actin.

The inhibitory effects of PTX2 were not as pronounced and with greater variability for smooth and non-muscle actin but nonetheless were significantly inhibited by PTX2. In contrast to the skeletal and cardiac actins, the smooth- and non-muscle actin used in the

current study both consisted of β- and γ-actin and studies have shown that filaments of these actins are less stable than those of sarcomeric α-actins (Khaitlina, 2001). Allen et al. (1996) found that the lengths of γ_{smooth} actin averaged less than half those of $\alpha_{skeletal}$ actin. Although they found that β-erythrocyte filaments were slightly longer than α-skeletal, they did not form viscoelastic gels as other actins did, indicating further differences. The lower stability of these isoactins, which may manifest as shorter, more fragile filaments, could result in a less efficient separation and quantification. Nonetheless, despite reduced sequence similarities (93.3% and 93.6%, respectively), relative to skeletal muscle actin, including substitution of Met-176 for leucine in the non-muscle β- and γ-actin isoform, the data illustrate inhibition of γ-smooth muscle and β- and γ- non-muscle actin polymerization by PTX2. However, the mixture of smooth muscle actin with both γ_{smooth} and $\beta_{non\text{-}muscle}$ complicates the interpretation. Nonetheless, based on the IC_{50} values for the various actin isoforms, the data suggest that amino acid variability at position 176 may be influencing inhibition by PTX2.

In vivo, PTX2, PTX1, and PTX6 are known to induce major histopathological alterations to the liver, with PTX2 also shown to adversely affect the spleen and kidneys (Ito et al., 2008; Munday, 2008; Yoon and Kim, 1997) with some gastrointestinal effects associated with PTX2 and PTX6 (Ito, 2006; Ito et al., 2008; Terao et al., 1986). *In vitro* studies that exposed heptatocytes, neuroblastoma cells, colorectal cells, and/or leukemia cells to PTX1, PTX2, and/or PTX6 revealed cytoskeletal changes prior to apoptotic cell death (Ares et al., 2007; Kim et al., 2008; Leira et al., 2002; Shin et al., 2008). Because of the ubiquitous inhibitory potential of PTX2 towards all actin isoforms, the results presented in the current study are consistent with all of these *in vivo* and *in vitro* studies. With the possible exception of the colorectal cells (likely dominated by γ_{smooth} muscle and $\beta_{cytoplasmic}$ actin), all other cell and tissue types employed or described in the previous PTX toxicity studies were likely dominated by non-muscle β- and γ-actin. Nonetheless, the current study shows that all actin isoforms are susceptible to inhibition of polymerization by PTX2. As such, the *in vivo* histopathological effects observed in the liver, kidneys, and spleen are likely a direct result of the PTX concentration at the target tissues. It is also possible that the symptoms observed are directly proportional to the inhibition of specific isoforms of actin. For instance, lethargy and lack of muscle coordination may be due to inhibition of skeletal muscle actin, whereas breathing difficulties and cyanosis (i.e., oxygen depletion) may have been due to inhibition of non-muscle actin in red blood cells and/or inhibition of cardiac muscle actin.

The inhibitory effects of PTX2 on actin appear to be restricted to polymerization and not depolymerization. Toxin-induced severing of actin filaments would have resulted in more ends from which G-actin could have dissociated followed by rapid depolymerization (Maciver et al., 1991; Saito et al., 1994). Collectively, our results are consistent with Allingham et al. (2007), whereby polymerization appears to be inhibited via disruption of the lateral contacts in F-actin filaments, capping the barbed end of a growing F-actin strand without severing the filaments.

At no time during the course of these studies did PTX2-SA alter the polymerization or depolymerization of any of the actin isoforms. PTX2-SA lacks an intact lactone ring providing evidence that the ring is fundamental to the toxicity of the PTX toxin class. This is consistent with cytoskeletal experiments performed with human neuroblastoma cells (Ares et al., 2007), *in vivo* studies in mice (Miles et al., 2006; Miles et al., 2004), and with examination of the contacts between PTX2 and skeletal actin in the crystal structure of Allingham et al. (2007). Our results thus lends further support to the non-assignment of a toxin equivalency factor (TEF) to PTX2-SA for regulatory purposes (EFSA, 2009).

Although PTX2 appears to be poorly absorbed from the gastrointestinal tract following oral exposure (Espenes et al., pers. comm.), it is clear that consumption of shellfish contaminated with PTXs will usually co-expose the organism to OA and DTXs that are produced by the same *Dinophysis* species. Since both OA and the DTXs toxins can dramatically disrupt and damage the gastrointestinal lining (Tubaro et al., 2004), there is the potential that uptake of PTXs may be enhanced.

In summary, we have shown that PTX2 causes a concentration-dependent decrease in both the rate and yield of skeletal muscle actin polymerization with no significant effects on depolymerization. The inhibitory effects of PTX2 appear to be conserved towards other actin isoforms (i.e., smooth muscle, cardiac muscle, and non-muscle) whereas no effects of PTX2 seco acid (up to 500 nM) were observed on actin polymerization, supporting previous findings that an intact lactone ring is necessary for bioactivity.

Conflict of interest statement

None.

Disclosure statement

The authors have no conflicts of interest.

Acknowledgement

The authors thank the Horace H. Rackham School of Graduate Studies and UM-D Office for Research and Sponsored Programs for financial support.

References

Allen, P.G., Shuster, C.B., Kas, J., Chaponnier, C., Janmey, P.A., Herman, I.M., 1996. Phalloidin binding and rheological differences among actin isoforms. Biochemistry 35, 14062–14069.

Allingham, J.S., Miles, C.O., Rayment, I., 2007. A structural basis for regulation of actin polymerization by pectenotoxins. J. Mol. Biol. 371, 959–970.

Allingham, J.S., Zampella, A., D'Auria, M.V., Rayment, I., 2005. Structures of microfilament destabilizing toxins bound to actin provide insight into toxin design and activity. PNAS 102, 14527–14532.

Ares, I.R., Louzao, M.C., Espina, B., Vieytes, M.R., Miles, C.O., Yasumoto, T., Botana, L.M., 2007. Lactone ring of pectenotoxins: a key factor for their activity on cytoskeletal dynamics. Cell. Physiol. Biochem. 19, 283–292.

Ares, I.R., Louzao, M.C., Vieytes, M.R., Yasumoto, T., Botana, L.M., 2005. Actin cytoskeleton of rabbit intestinal cells is a target for potent marine phycotoxins. J. Exp. Biol. 208, 4345–4354.

Bialojan, C., Takai, A., 1988. Inhibitory effect of a marine-sponge toxin, okadaic acid, on protein phosphatases. Biochem. J. 256, 283–290.

Brooks, F.J., Carlsson, A.E., 2008. Actin polymerization overshoots and ATP hydrolysis as assayed by pyrene fluorescence. Biophys. J. 95, 1050–1062.

Cooper, J.A., 1987. Effects of cytochalasin and phalloidin on actin. J. Cell Biol. 105, 1473–1478.

SA, E.F., 2009. Marine biotoxins in shellfish – Pectenotoxin group: Scientific Opinion of the Panel on Contaminants in the Food chain. The EFSA Journal 1109, 1–47.

Espina, B., Rubiolo, J.A., 2008. Marine toxins and the cytoskeleton: pectenotoxins, unusual macrolides that disrupt actin. FEBS J. 275, 6082–6088.

Faulstich, H., Zobeley, S., Heintz, D., Drewes, G., 1993. Probing the phalloidin binding site of actin. FEBS Letters 318, 218–222.

Fladmark, K.E., Serres, M.H., Larsen, N.L., Yasumoto, T., Aune, T., Doskeland, S.O., 1998. Sensitive detection of apoptogenic toxins in suspension cultures of rat and salmon hepatocytes. Toxicon 36, 1101–1114.

Hori, M., Matsuura, Y., Yoshimoto, R., Ozaki, H., Yasumoto, T., Karaki, H., 1999. Actin depolymerizing action by marine toxin, pectenotoxin-2. Nippon Yakurigaku Zasshi 114, 225P–229P.

Ishige, M., Satoh, N., Yasumoto, T., 1988. Pathological studies on mice administered with the causative agent of diarrhetic shellfish poisoning (okadaic acid and pectenotoxin-2). Hokkaidoritsu Eisei Kenkyushoho 18, 15–18.

Ito, E., 2006. Verification of diarrhetic activities of PTX-2 and okadaic acid *in vivo*, 12th International Conference on Harmful Algae, Copenhagen, Denmark., pp. 198 (abstract).

Ito, E., Suzuki, T., Oshima, Y., Yasumoto, T., 2008. Studies of diarrhetic activity on pectenotoxin-6 in the mouse and rat. Toxicon 51, 707–716.

Khaitlina, S.Y., 2001. Functional specificity of actin isoforms. In: Jeon, K.W. (Ed.), Int Rev Cytol, 2000/11/04 ed. Academic Press, San Diego, pp. 35–98.

Kim, G.-Y., Kim, W.-J., Choi, Y.H., 2011. Pectenotoxin-2 from marine sponges: a potential anti-cancer agent—a Review. Marine Drugs 9, 2176–2187.

Kim, M.O., Moon, D.O., Heo, M.S., Lee, J.D., Jung, J.H., Kim, S.K., Choi, Y.H., Kim, G.Y., 2008. Pectenotoxin-2 abolishes constitutively activated NF-kappaB, leading to suppression of NF-kappaB related gene products and potentiation of apoptosis. Cancer Lett. 271, 25–33.

Laemmli, U.K., 1970. Cleavage of structural proteins during the assembly of the head of bacteriophage T4. Nature 227, 680–685.

Leira, F., Cabado, A.G., Vieytes, M.R., Roman, Y., Alfonso, A., Botana, L.M., Yasumoto, T., Malaguti, C., Rossini, G.P., 2002. Characterization of F-actin depolymerization as a major toxic event induced by pectenotoxin-6 in neuroblastoma cells. Biochem. Pharmacol. 63, 1979–1988.

Maciver, S.K., Zot, H.G., Pollard, T.D., 1991. Characterization of actin filament severing by actophorin from *Acanthamoeba castellanii*. J. Cell Biol. 115, 1611–1620.

Miles, C.O., Wilkins, A.L., Munday, J.S., Munday, R., Hawkes, A.D., Jensen, D.J., Cooney, J.M., Beuzenberg, V., 2006. Production of 7-*epi*-pectenotoxin-2 seco acid and assessment of its acute toxicity to mice. J. Agric. Food Chem. 54, 1530–1534.

Miles, C.O., Wilkins, A.L., Munday, R., Dines, M.H., Hawkes, A.D., Briggs, L.R., Sandvik, M., Jensen, D.J., Cooney, J.M., Holland, P.T., Quilliam, M.A., MacKenzie, A.L., Beuzenberg, V., Towers, N.R., 2004. Isolation of pectenotoxin-2 from *Dinophysis acuta* and its conversion to pectenotoxin-2 seco acid, and preliminary assessment of their acute toxicities. Toxicon 43, 1–9.

Munday, J.S., 2008. Toxicology of the Pectenotoxins. In: Botana, L.M. (Ed.), Seafood and Freshwater toxins: Pharmacology, Physiology, and Detection, 2nd ed. CRC Press (Taylor and Francis Group). Boca Raton, FL, pp. 371–380.

Saito, S., Watabe, S., Ozaki, H., Fusetani, N., Karaki, H., 1994. Mycalolide B, a novel actin depolymerizing agent. J. Biol. Chem. 269, 29710–29714.

Sandvik, M., Fæste, C., Rundberget, T., Flåøyen, A., Miles, C.O., Petersen, D., 2004. *In vitro* biotransformations of algal toxins, 5th International Conference on Molluscan Shellfish Safety. Galway, Ireland, pp. 162.

Sasaki, K., Wright, J.L., Yasumoto, T., 1998. Identification and characterization of pectenotoxin (PTX) 4 and PTX7 as spiroketal stereoisomers of two previously reported pectenotoxins. J. Org. Chem. 63, 2475–2480.

Shin, D.Y., Kim, G.Y., Kim, N.D., Jung, J.H., Kim, S.K., Kang, H.S., Choi, Y.H., 2008. Induction of apoptosis by pectenotoxin-2 is mediated with the induction of DR4/DR5, Egr-1 and NAG-1, activation of caspases and modulation of the Bcl-2 family in p53-deficient Hep3B hepatocellular carcinoma cells. Oncol. Rep. 19, 517–526.

Suzuki, T., Walter, J.A., LeBlanc, P., MacKinnon, S., Miles, C.O., Wilkins, A.L., Munday, R., Beuzenberg, V., MacKenzie, A.L., Jensen, D.J., Cooney, J.M., Quilliam, M.A., 2006. Identification of pectenotoxin-11 as 34*S*-hydroxypectenotoxin-2, a new pectenotoxin analogue in the toxic dinoflagellate *Dinophysis acuta* from New Zealand. Chem. Res. Toxicol. 19, 310–318.

Takai, A., Murata, M., Torigoe, K., Isobe, M., Mieskes, G., Yasumoto, T., 1992. Inhibitory effect of okadaic acid derivatives on protein phosphatases. a study on structure-affinity relationship. Biochem. J. 284 (Pt 2), 539–544.

Terao, K., Ito, E., Yanagi, T., Yasumoto, T., 1986. Histopathological studies on experimental marine toxin poisoning. 1. ultrastructural changes in the small intestine and liver of suckling mice induced by dinophysistoxin-1 and pectenotoxin-1. Toxicon 24, 1141–1151.

Tubaro, A., Sosa, S., Altinier, G., Soranzo, M.R., Satake, M., Della Loggia, R., Yasumoto, T., 2004. Short-term oral toxicity of homoyessotoxins, yessotoxin and okadaic acid in mice. Toxicon 43, 439–445.

Yasumoto, T., Murata, M., Oshima, Y., Sano, M., Matsumoto, G., Clardy, J., 1985. Diarrhetic shellfish toxins. Tetrahedron 41, 1019–1025.

Yoon, M.Y., Kim, Y.C., 1997. Acute toxicity of pectenotoxin 2 and its effects on hepatic metabolizing enzyme system in mice. Korean J. Toxicol. 13, 183–186.

Zhou, Z.H., Komiyama, M., Terao, K., Shimada, Y., 1994. Effects of pectenotoxin-1 on liver cells *in vitro*. Nat. Toxins 2, 132–135.